Empowering antimicrobial photodynamic therapy of Staphylococcus aureus infections with potassium iodide

Bispo, Mafalda; Suhani, Sabrina; van Dijl, Jan Maarten

Published in:
Journal of Photochemistry and Photobiology B: Biology

DOI:
10.1016/j.jphotobiol.2021.112334

Publication date:
2021

Journal of Photochemistry & Photobiology, B: Biology 225 (2021) 112334

Contents lists available at ScienceDirect

Journal of Photochemistry & Photobiology, B: Biology

journal homepage: www.elsevier.com/locate/jphotobiol

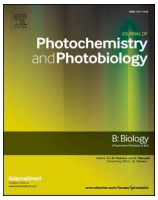

Empowering antimicrobial photodynamic therapy of *Staphylococcus aureus* infections with potassium iodide

Mafalda Bispo, Sabrina Suhani, Jan Maarten van Dijl *

Department of Medical Microbiology, University of Groningen, University Medical Center Groningen, Hanzeplein 1, 9713 GZ, Groningen, The Netherlands

ARTICLE INFO

Keywords:
Staphylococcus aureus
Antimicrobial photodynamic therapy
Human serum albumin
Antioxidant response
Potassium iodide

ABSTRACT

Infections caused by the Gram-positive bacterium *Staphylococcus aureus*, especially methicillin-resistant *S. aureus* (MRSA), impose a great burden on global healthcare systems. Thus, there is an urgent need for alternative approaches to fight staphylococcal infections, such as targeted antimicrobial photodynamic therapy (aPDT). We recently reported that targeted aPDT with the *S. aureus*-specific immunoconjugate 1D9-700DX can be effectively applied to eradicate MRSA. Nonetheless, the efficacy of aPDT in the human body may be diminished by powerful antioxidant activities. In particular, we observed that the efficacy of aPDT with 1D9-700DX towards MRSA was reduced in human plasma. Here we show that this antagonistic effect can be attributed to human serum albumin, which represents the largest pool of free thiols in plasma for trapping reactive oxygen species. Importantly, we also show that our targeted aPDT approach with 1D9-700DX can be empowered by the non-toxic inorganic salt potassium iodide (KI), which reacts with the singlet oxygen produced upon aPDT, resulting in the formation of free iodine. The targeted iodine formation allows full eradication of MRSA (more than 6-log reduction) without negatively affecting other non-targeted bacterial species or human cells. Altogether, we show that the addition of KI allows a drastic reduction of both the amount of the immunoconjugate 1D9-700DX and the irradiation time needed for effective elimination of MRSA by aPDT in the presence of human serum albumin.

1. Introduction

The Gram-positive bacterium *Staphylococcus aureus* is a powerful human pathogen that causes diseases ranging from relatively minor skin infections to severe and life-threating infections such as pneumonia, endocarditis and sepsis [1]. Nosocomial infections caused by *S. aureus* pose a considerable burden on global healthcare systems, especially the methicillin-resistant *S. aureus* (MRSA) [2]. Being resistant to β-lactam antibiotics, MRSA is a particularly serious threat to frail and immunocompromised individuals [3]. Considering the substantial morbidity and mortality associated with this bacterium, along with the declining efficacy of available treatment measures, there is an urgent need to identify alternative strategies to treat MRSA infections.

Antimicrobial photodynamic therapy (aPDT) has recently gained attention because of its efficacy against a wide range of pathogens, the multi-target mechanism of action, the possibility to eradicate biofilms and the apparent absence of resistance [4,5]. aPDT relies on the generation of reactive oxygen species (ROS), particularly singlet oxygen ($^1O_2$), upon exposure of a photo-activable antimicrobial drug, referred to as photosensitizer and to light of a suitable wavelength. The generated ROS can thereafter cause oxidative damage to various essential cellular components, leading to bacterial death. The absence of resistance to aPDT can be attributed to the relatively short treatment times, which do not allow the bacteria to harness effective survival mechanisms [6–8]. Importantly, by covalently conjugating a suitable photosensitizer to a bacteria-targeted delivery vehicle, it is possible to minimize possible collateral damage to neighbouring cells [9]. Nonetheless, in view of the indiscriminate cytotoxicity of ROS, it is important to explore therapeutic windows in which pathogens are inactivated by aPDT without causing harm to the surrounding tissues or disturbing the local microenvironment. To this end, it is necessary to define the optimal concentration of the targeted aPDT agent and the light dose applied.

Conserved proteins exposed on the bacterial cell surface are attractive potential targets for targeted aPDT [10]. The immunodominant *S. aureus* antigen A (IsaA) is a non-covalently cell wall-attached protein recognized by immunoglobulins (IgGs) from both *S. aureus* carriers and non-carriers [11,12]. Moreover, proteomic analysis of the *S. aureus* exoproteome showed that IsaA is invariantly produced by all

* Corresponding author at: Department of Medical Microbiology, University of Groningen, University Medical Center Groningen, Hanzeplein 1, 9700 RB Groningen, The Netherlands
E-mail address: j.m.van.dijl01@umcg.nl (J.M. van Dijl).

https://doi.org/10.1016/j.jphotobiol.2021.112334
Received 22 August 2021; Received in revised form 26 September 2021; Accepted 7 October 2021
Available online 13 October 2021

investigated isolates of this pathogen [13–15]. The appealing properties of this *S. aureus* antigen prompted the development of monoclonal antibodies (mAbs) against it [16–18], among which the fully human IgG1 designated 1D9. In previous studies, 1D9 has been labelled with fluorescent dyes or radionuclides for the rapid and non-invasive diagnosis of *S. aureus* soft tissue infections as well as spinal and shoulder implant infections in mice using positron emission tomography–computed tomography (PET-CT) or in vivo fluorescence imaging [19–21]. This mAb was also previously conjugated with a silicon-phthalocyanine derivative (IRDye 700DX) for the targeted aPDT of *S. aureus* infections [22]. IRDye 700DX has a strong absorption band in the near-infrared (NIR) region of the spectrum [23], and it has been recently clinically approved in Japan for PDT of inoperable head and neck cancers in patients [24,25]. The *S. aureus*-specific immunoconjugate 1D9-700DX can successfully eradicate high loads of bacteria in vitro and destroy the surface of a bacterial biofilm [22]. Furthermore, aPDT with 1D9-700DX improved the survival of MRSA-infected larvae of the wax moth *Galleria mellonella* [22].

A potential limitation for translating aPDT to clinical applications relates to the natural protective antioxidant mechanisms in the human body. In particular, we have previously observed that human plasma can interfere with effective 1D9-700DX-mediated aPDT. Importantly, this antioxidant effect may be overcome in the presence of potassium iodide (KI) [22], a non-toxic inorganic salt capable of forming free iodine upon reaction with the $^1O_2$ generated through red light activation of the conjugated IRDye 700DX. Consequently, KI has the potential to promote increased *S. aureus* killing rates upon aPDT with 1D9-700DX [26,27].

The present study was aimed at investigating whether human serum albumin (HSA) contributes to the aPDT-antagonizing effect of human plasma and, if so, how KI can be applied to overcome the antioxidant activity of HSA. To this end, we followed the approaches schematically outlined in Fig. 1. HSA is the most abundant protein in plasma and its two sulphur-containing methionine and cysteine residues were previously shown to trap free radical activity in serum [28,29]. Here we show that blocking of the conserved Cys-34 residue with the alkylating agents iodoacetamide (IAA) or N-ethylmaleimide (NEM) overcomes the antioxidant activity of both human and bovine serum albumin. Importantly, we also show that KI allows effective aPDT of MRSA in the presence of HSA without loss of the staphylococcal target specificity.

2. Results

2.1. Serum Albumin Antagonizes aPDT with 1D9-700DX

Conceivably, there are at least two possible mechanisms that can limit targeted aPDT with 1D9-700DX in human plasma. In the first place, the human plasma has antioxidant activity to preclude potentially detrimental effects of ROS. Such antioxidant activity can limit the efficacy of aPDT with 1D9-700DX in the treatment of *S. aureus* infections [22]. Secondly, the stability of 1D9-700DX could be affected by plasma proteases or secreted bacterial proteases [30]. To assess the latter possibility, we first incubated the 1D9-700DX immunoconjugate in plasma for 90 min and examined its stability by lithium dodecyl sulphate (LDS) PAGE. As shown in Fig. S1, incubation in plasma had no impact on the amount and integrity of 1D9-700DX, and the same was true when this immunoconjugate was preincubated with *S. aureus*. To determine whether the antioxidant activity of serum albumin could be responsible for the antagonizing effect of human plasma towards aPDT with 1D9-700DX, we investigated the effect of different concentrations of HSA on the aPDT efficacy of 1D9-700DX using the community-acquired MRSA (CA-MRSA) strain AH4807 as the target bacterium. In parallel, native bovine serum albumin (BSA) was used as a control. In the absence of these serum albumins, 3.3 μM of 1D9-700DX reduced the number of colony-forming units (CFU) in the initial bacterial inoculum by approximately 3-log units upon 5 min irradiation with red light of 690 nm at 30 J·cm^{-2} (100 mW·cm^{-2}; Fig. 2), which is in full accordance with the results from our previous studies [22]. This observation is important, because at least a 3-log reduction in the number of viable bacteria (i.e. 99.9% bacterial killing) should be achieved for adequate antimicrobial activity [31]. However, in the presence of 1.3 mg·mL^{-1} of either BSA or HSA, the aPDT efficacy of 1D9-700DX was reduced significantly, and at a concentration of 2.5 mg·mL^{-1} of either serum albumin bacterial killing by aPDT was no longer detectable (Fig. 2).

2.2. Free Thiols of Serum Albumin Antagonize aPDT with 1D9-700DX

A possible involvement of the unique Cys-34 of HSA and BSA in the interference with aPDT was assessed by its targeted modification with the thiol alkylating agents IAA or NEM (Fig. 3). Of note, both IAA and

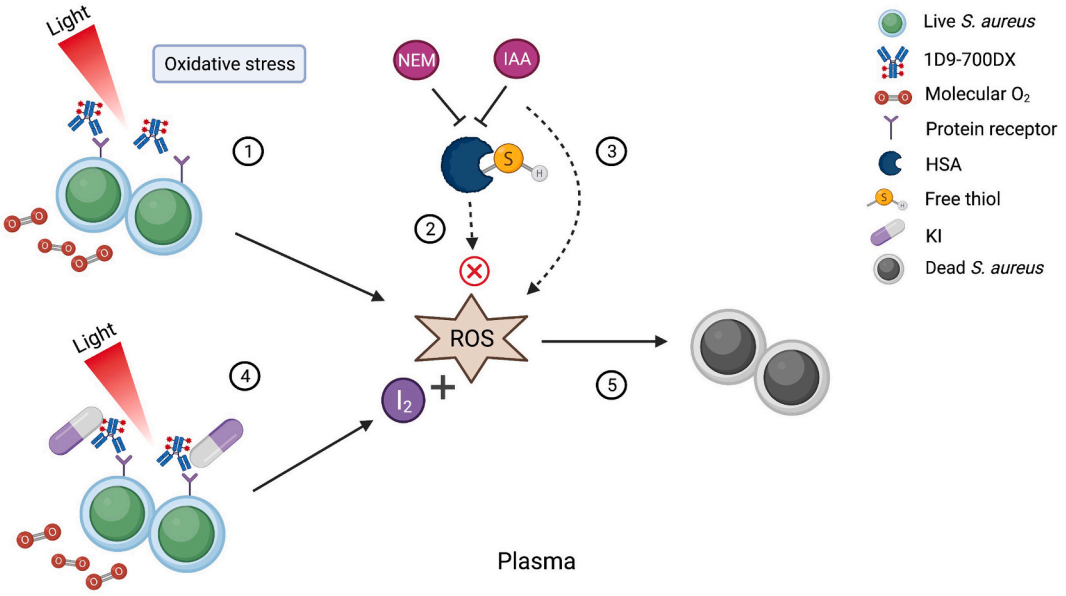

Fig. 1. Summary graphic illustration. **1.** aPDT with 1D9-700DX against *S. aureus* in human plasma. **2.** Reduced thiols of HSA have an aPDT-antagonizing antioxidant activity. **3.** Alkylating agents (NEM and IAA) block the free thiols of HSA and restore aPDT. **4.** aPDT with 1D9-700DX in the presence of KI leads to the production of iodine (I_2) due to ROS generation. **5.** The combined effects of ROS and I_2 overcome the antioxidant activity of HSA, and allow effective killing of *S. aureus* by aPDT. This figure is created with BioRender.com.

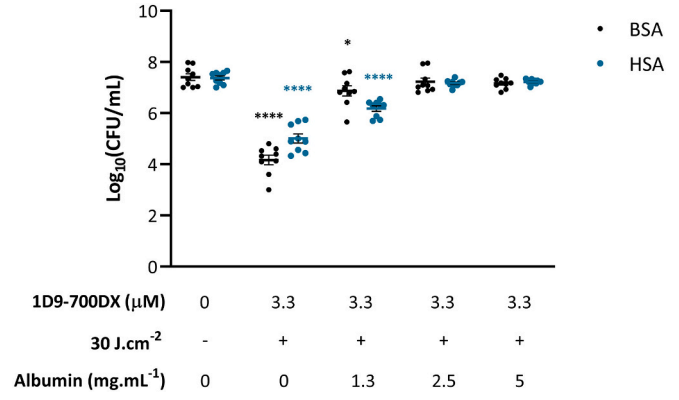

Fig. 2. Antioxidant properties of BSA and HSA counteract aPDT of MRSA. Photo-activated killing of ~1 × 10^7 CFU/mL of CA-MRSA AH4807 grown to exponential phase, in the presence or absence of different concentrations of BSA or HSA, with or without 3.3 μM of 1D9-700DX and with or without red light exposure (30 J·cm^{-2}). Numbers of surviving bacteria (Log_{10}[CFU/mL]) are represented in the Figure. Data are presented as the mean ± SEM of three independent experiments performed in triplicates. Two-way ANOVA with subsequent Dunnett's multiple-comparison tests were used for statistical analysis. Significant differences compared with the control group (no photosensitizer, no light and no serum albumin) are marked with blue asterisks as follows: *P < 0.03; ****P < 0.0001. Note that the experiments with BSA or HSA were performed on different dates with different batches of 1D9-700DX, which explains the variation in CFU counts observed in the absence of BSA or HSA. (For interpretation of the references to colour in this figure legend, the reader is referred to the web version of this article.)

NEM act as irreversible inhibitors of catalytic Cys residues by alkylating their reduced thiol side groups [32]. Since IAA can by itself be toxic for bacteria due to interference with the bacterial defences against oxidative stress [33], we first verified that treatment of the CA-MRSA bacteria with IAA concentrations up to 3 mg·mL^{-1} in the dark or upon exposure to red light had no effect on their viability (Fig. 3A). Next, we verified the effects of IAA upon aPDT with 1D9-700DX. This revealed that concentrations of IAA higher than 1.5 mg·mL^{-1} combined with 1D9-700DX killed 100% of the initial bacterial inoculum upon red light irradiation (Fig. 3A). We attribute the latter toxic effect of IAA to an impaired capacity of the bacteria to cope with the ROS generated by aPDT, since also the free thiols of bacterial antioxidants can be blocked by IAA. For instance, this applies to low molecular weight thiols and thiol-disulphide oxidoreductases employed by *S. aureus* to detoxify ROS [33].

After assessing the toxicity of IAA towards CA-MRSA with or without aPDT with 1D9-700DX, we investigated whether IAA could restore the bacterial killing by aPDT in the presence of serum albumins. Indeed, as shown in Fig. 3B, 0.8 mg·mL^{-1} of IAA was sufficient to restore bacterial killing by aPDT in the presence of 1.3 mg·mL^{-1} BSA or HSA, which is an albumin concentration that significantly limits aPDT with 1D9-700DX (Fig. 2). Although BSA and HSA are very similar proteins [34], IAA was more efficient in antagonizing the antioxidant properties of BSA than those of HSA (Fig. 3B). Conceivably, this difference relates to slightly different oxidation states of the BSA and HSA provided by our commercial supplier. For instance, Cys-34 of serum albumins is able to form disulphide bonds with small compounds with sulfhydryl groups (e.g. cysteine, homocysteine or glutathione) [35], and our BSA and HSA preparations could thus be oxidized to different extents. In turn, this would result in a differential blocking efficacy by IAA [35].

To verify these observations with another alkylating agent, we used NEM. Since NEM is also known to be toxic for bacteria due to the inactivation of important antioxidant pathways that involve free thiols and the consequent interference with the bacterial ability to cope with ROS [36], we first investigated which levels of NEM can be tolerated by CA-MRSA. To assess this, the bacteria were treated with different concentrations of NEM in the dark and the viability was measured by plating and subsequent CFU-counting. Significant NEM toxicity towards CA-MRSA was observed at NEM concentrations of 1 mg·mL^{-1} and higher, with 100% bacterial killing at 3 mg·mL^{-1} (Fig. 3C). Thus, a NEM concentration of 0.3 mg·mL^{-1} and a slightly lowered concentration of 1D9-700DX (1.5 μM) were chosen for aPDT studies in the presence of HSA. To this end, CA-MRSA was incubated with 1D9-700DX in combination with HSA and/or NEM, and the samples were either irradiated with red light at 30 J·cm^{-2} or kept in the dark. As shown in Fig. 3D, the antioxidant effect of HSA was blocked by NEM and the aPDT effect of red light-activated 1D9-700DX was restored. These findings are fully consistent with the role of Cys-34 in the aPDT-antagonizing activity of serum albumins. To verify this conclusion, we measured the concentration of free thiols in our HSA preparation before and after NEM treatment using the Ellman's assay. In this assay, the reagent 5,5′-dithio-bis-(2-nitrobenzoic acid) (DTNB) reacts with free sulfhydryl groups to yield 2-nitro-5-thiobenzoic acid, which absorbs light at 412 nm [37]. As shown in **Fig. S2**, the concentration of free thiols in HSA solutions is significantly reduced in the presence of 1.2 mg·mL^{-1} NEM. This explains the reduced antioxidant activity of HSA under this condition, albeit that this concentration of NEM was higher than in the experiment shown in Fig. 3D and might result in a higher level of free thiol blocking in HSA.

2.3. aPDT with 1D9-700DX in the Presence of Potassium Iodide Overcomes the Antioxidant Response of HSA

KI is an inorganic salt that can be applied to enhance the bactericidal effect of aPDT in human plasma due to $^1O_2$-mediated iodine formation [22,38]. We therefore explored whether KI can help to fine-tune the targeted aPDT with 1D9-700DX to minimize the concentration of this immunoconjugate and the time of irradiation required to eliminate CA-MRSA. In turn, this would ensure minimal collateral damage to non-targeted host cells and the microbiota [39]. To this end, we first exposed CA-MRSA to 1.5 μM of 1D9-700DX and red light, and assessed the bactericidal effect in the presence of increasing concentrations of KI (Fig. 4A). Here it should be noted that we have previously shown that a KI concentration of 50 mM is not toxic to the bacteria [22]. At KI concentrations of 15 μM and higher, we observed enhanced bacterial killing by red light-activated 1D9-700DX. At 30 μM KI, the CA-MRSA was completely eradicated, which corresponds to an enhanced aPDT efficacy by more than 6-log units compared to aPDT in the absence of KI. In this respect, it is important to note that according to the 'Association of Official Analytical Chemicals' (AOAC), it is recommended that the mean log density for *S. aureus* needs to be at least 6 when testing a disinfectant [40]. We have previously shown that the concentration of 1D9-700DX that kills 100% of the initial bacteria after aPDT in the absence of KI is 9.8 μM [22]. The present data shows that, in the presence of KI, the same effect can be achieved with a concentration of 1D9-700DX that is 6-fold lower (Fig. 4A). To evaluate whether it is also possible to shorten the time of irradiation with red light at a power of 100 mW·cm^{-2}, CA-MRSA was incubated with 1.5 μM 1D9-700DX and a slightly increased KI concentration of 120 μM. Thereafter, the bacteria were irradiated with red light for different periods of time (1 to 5 min). Importantly, it took merely 2 min of irradiation to completely eradicate the CA-MRSA inoculum by aPDT with 1D9-700DX in the presence of KI (Fig. 4B). The data presented in Fig. 4A–B therefore demonstrate that KI significantly enhances the efficacy of aPDT. This prompted us to investigate whether KI can also help to overcome the antioxidant properties of HSA. Fig. 4C shows that this is indeed the case as, by the combined use of 1D9-700DX and KI, a significant CFU reduction of CA-MRSA was achieved upon irradiation with red light (30 J·cm^{-2}), in the presence of HSA.

2.4. Targeted aPDT with 1D9-700DX Combined with KI has no side Effects Towards Gram-negative Bacteria in a Co-culture

The 1D9 mAb specifically binds to the IsaA protein present on the *S. aureus* cell wall [18]. As a first approach to investigate the target

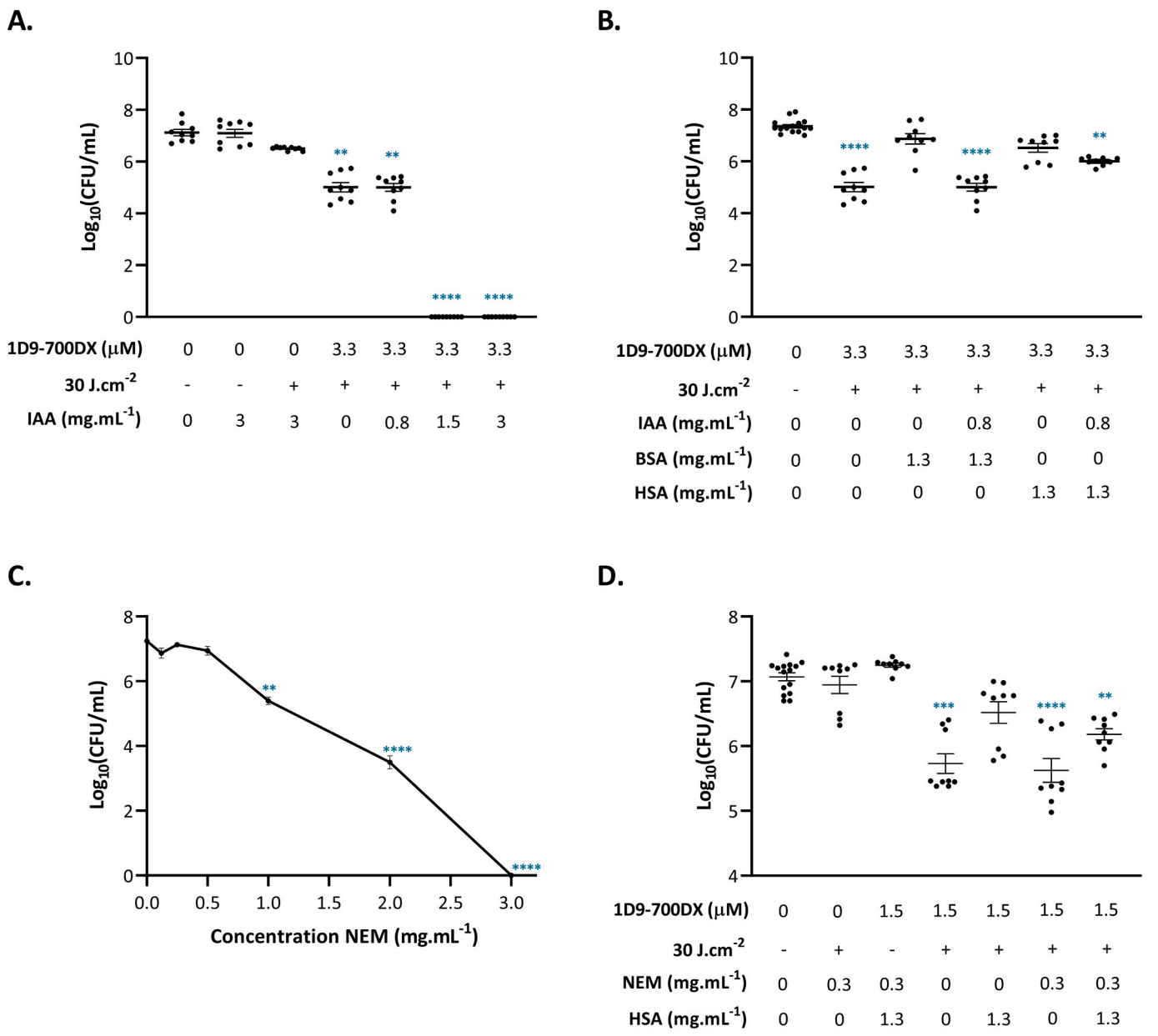

Fig. 3. Blocking free thiols of albumins with alkylating agents. Toxicity dose response of NEM and IAA towards CA-MRSA AH4807 grown to exponential phase. ~1 × 10^7 CFU/mL were incubated with or without IAA (**A**) or NEM (**C**) and with 1D9-700DX or PBS. The bacteria were either irradiated with red light (30 J·cm^{-2}) or kept in the dark. Surviving numbers of bacteria are represented in Log_{10}(CFU/mL). aPDT efficacy of 1D9-700DX was restored in the presence of BSA or HSA after blocking the free thiols of these serum albumins with IAA (**B**) or NEM (**D**) at concentrations of 0.8 mg·mL^{-1} or 0.3 mg·mL^{-1}, respectively. Data are presented as the mean ± SEM of three independent experiments performed in triplicates. Kruskal-Wallis tests with subsequent Dunn's multiple-comparison tests were used for statistical analysis. Significant differences compared with the control group (no photosensitizer, no light, no IAA/NEM and no serum albumin) are marked with blue asterisks as follows: $^{**}P < 0.002$; $^{***}P < 0.0002$; $^{****}P < 0.0001$. (For interpretation of the references to colour in this figure legend, the reader is referred to the web version of this article.)

specificity of 1D9-700DX for *S. aureus*, we applied a co-culture model where *S. aureus* was co-cultured with the Gram-negative bacterium *K. oxytoca*. These two bacteria were previously shown to co-exist in chronic wounds of patients with the genetic blistering disease epidermolysis bullosa (EB) and, accordingly, they can be readily co-cultured in broth and on plate [41]. Fig. 5 shows that aPDT with 1D9-700DX completely eradicated the *S. aureus* strain, both in the mono- and co-cultures, while *K. oxytoca* remained unaffected. Moreover, the presence of KI and the resulting production of iodine reactive species upon aPDT with 1D9-700DX, did not affect the viability of *K. oxytoca*, neither in mono- nor in co-culture. This shows that *S. aureus*-targeted aPDT with 1D9-700DX in the presence of KI still selectively addresses the staphylococcal antigen IsaA, without negative effects of the concomitant iodine formation on non-targeted bacterial cells.

2.5. 1D9-700DX Combined with KI Selectively Kills MRSA Without Damaging Mammalian Cells

We previously demonstrated that aPDT with 1D9-700DX was not toxic to the human cervical cancer HeLa cell line at concentrations below 0.7 μM, without wash of the unbound immunoconjugate [22]. However, this concentration of 1D9-700DX is not effective in the elimination of high loads of bacteria upon red light activation [22]. We therefore decided to investigate whether, in a co-culture of HeLa cells

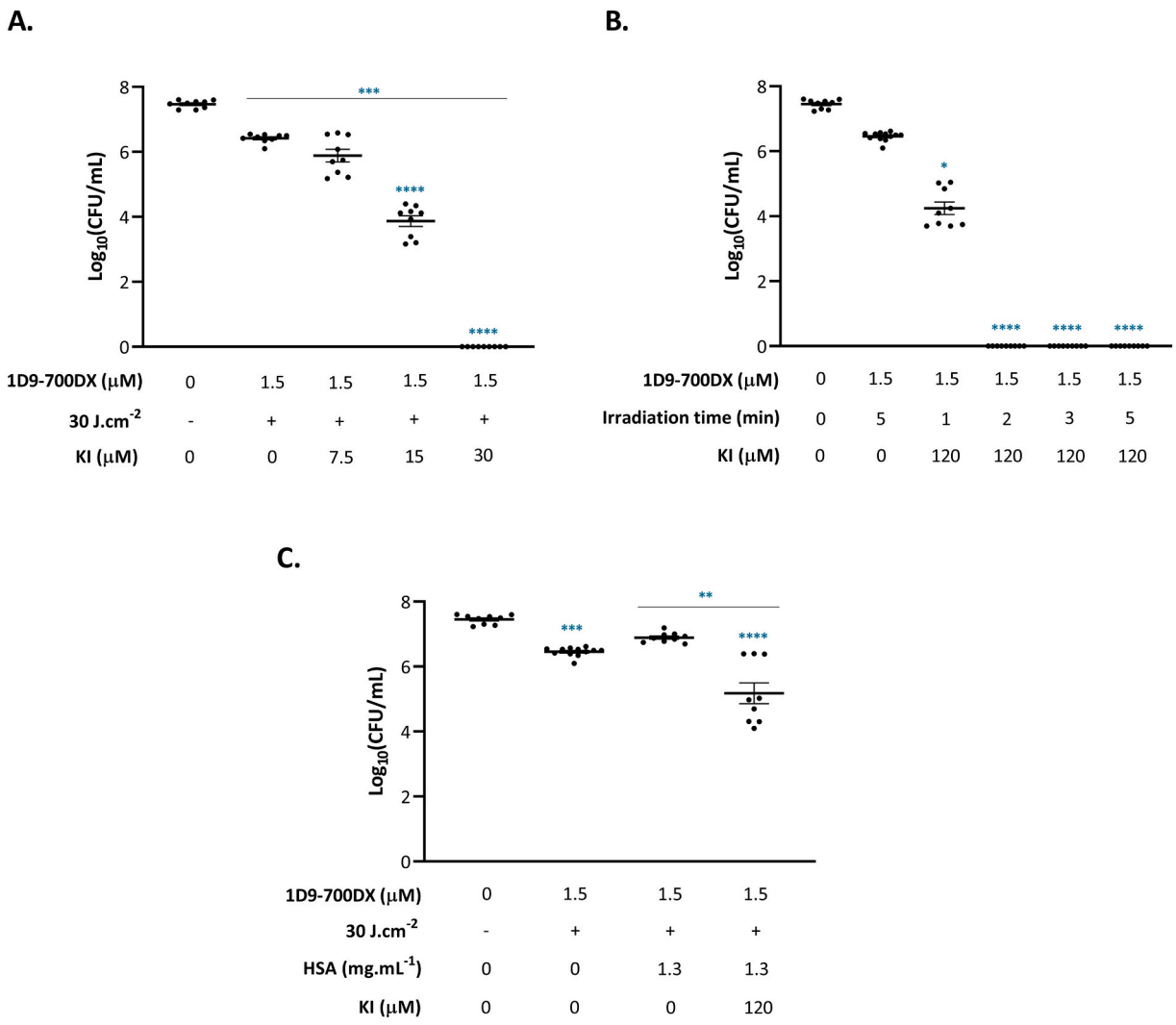

Fig. 4. KI empowers 1D9-700DX-mediated aPDT and overcomes antioxidant activity of HSA. CA-MRSA AH4807 was grown to exponential phase and ~ 1×10^7 CFU/mL were incubated with or without KI (7.5, 15 and 30 μM) (**A**), KI 120 μM (**B** and **C**) and/or 1.3 mg·mL^{-1} HSA (**C**). Photo-activated killing was assessed by incubating the bacteria with or without 1.5 μM of 1D9-700DX in the presence or absence of light (30 J.cm^{-2}). Numbers of surviving bacteria (Log_{10}[CFU/mL]) are represented in the figures. Data are presented as the mean ± SEM of three independent experiments performed in triplicates. Kruskal-Wallis tests with subsequent Dunn's multiple-comparison tests were used for statistical analysis. Significant differences compared with the control group (no photosensitizer, no light, no KI and no HSA) are marked with blue asterisks as follows: * $P < 0.03$; ** $P < 0.002$; *** $P < 0.0002$; **** $P < 0.0001$. (For interpretation of the references to colour in this figure legend, the reader is referred to the web version of this article.)

and *S. aureus*, aPDT with 1D9-700DX in the presence of KI allows the selective killing of high loads of *S. aureus* without damaging the mammalian cells. To this end, we firstly assessed the possible cytotoxicity of KI towards HeLa cells. The cell viability in the presence of increasing concentrations of KI was evaluated with a colorimetric assay based on the reduction of the yellow 3-(4,5-Dimethylthiazol-2-yl)-2,5-Diphenyltetrazolium Bromide (MTT) by mitochondrial dehydrogenase activity to a purple formazan precipitate. Accordingly, the reduction of MTT is directly correlated with the metabolic activity of living cells [42]. The MTT assays showed that concentrations of KI equal or lower than 50 mM were not toxic to HeLa cells (**Fig. S3**). Next, we performed co-culture experiments where HeLa cells were infected with 3×10^6 CFU/mL of CA-MRSA and, subsequently, incubated for 30 min with a low dose of 1D9-700DX (0.2 μM) with or without KI (50 mM). The co-cultures were then irradiated with red light (30 J·cm^{-2}), and the viability of extracellular bacteria and HeLa cells was assessed by CFU counting and MTT assays. This showed that the bacterial viability was reduced by approximately 60% after aPDT with 1D9-700DX in the absence of KI. In contrast, a 95% reduction in the CFU counts was observed when aPDT with 1D9-700DX was performed in the presence of KI (Fig. 6A). Importantly, these treatments had no negative repercussions for the viability of the HeLa cells as measured by MTT reduction (Fig. 6B). We therefore conclude that targeted aPDT with 1D9-700DX combined with the administration of KI can specifically kill *S. aureus*, and that the produced ROS and iodine are specifically addressed to the bacterial cells by using the 1D9 mAb as a targeting agent to avoid collateral damage of nearby mammalian cells.

3. Discussion

The treatment of *S. aureus* infections remains an important clinical challenge due to this pathogen's ability to acquire high resistance to antimicrobial agents. This calls for the development of novel, alternative strategies to fight this persistent pathogen. In the present study, we focused attention on aPDT of MRSA infections with a conjugate of the human mAb 1D9 and the NIR photosensitizer IRDye 700DX. We have previously shown that the immunoconjugate 1D9-700DX specifically binds to the staphylococcal surface protein IsaA and, upon activation

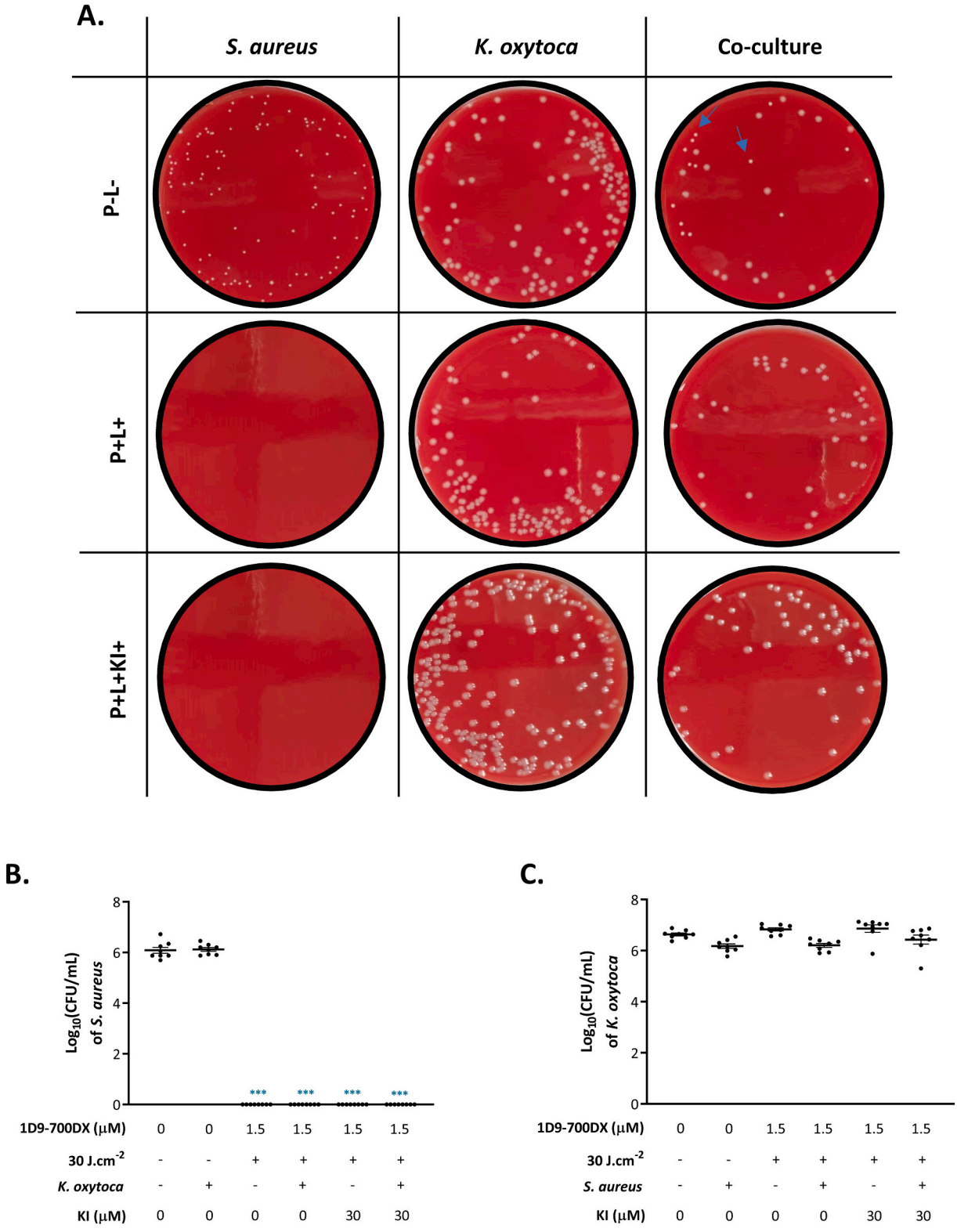

Fig. 5. Specific toxicity of aPDT with 1D9-700DX combined with KI towards *S. aureus* in a co-culture with *K. oxytoca*. Photo-activated killing was assessed by incubating *S. aureus* and or *K. oxytoca* with or without 1.5 µM 1D9-700DX in the presence or absence of KI 30 µM. Bacteria were either kept in the dark or irradiated with 30 J·cm^{-2} of red light. After 16 h on BA plates at 37 °C, *S. aureus* forms relatively small colonies, while *K. oxytoca* forms distinctive colonies that are relatively large. Some typical *S. aureus* colonies are marked with a blue arrow in the co-culture plates (**A**). Numbers of surviving bacteria (Log$_{10}$[CFU/ mL]) of *S. aureus* and *K. oxytoca* are represented in panels **B** and **C**, respectively, representing either the mono- or co-culture conditions. Data are presented as the mean ± SEM of three independent experiments performed in triplicates. Kruskal-Wallis tests with subsequent Dunn's multiple-comparison tests were used for statistical analysis. Significant differences compared with the control group (no photosensitizer, no light and no KI) are marked with blue asterisks as follows: ***$P < 0.0002$. (For interpretation of the references to colour in this figure legend, the reader is referred to the web version of this article.)

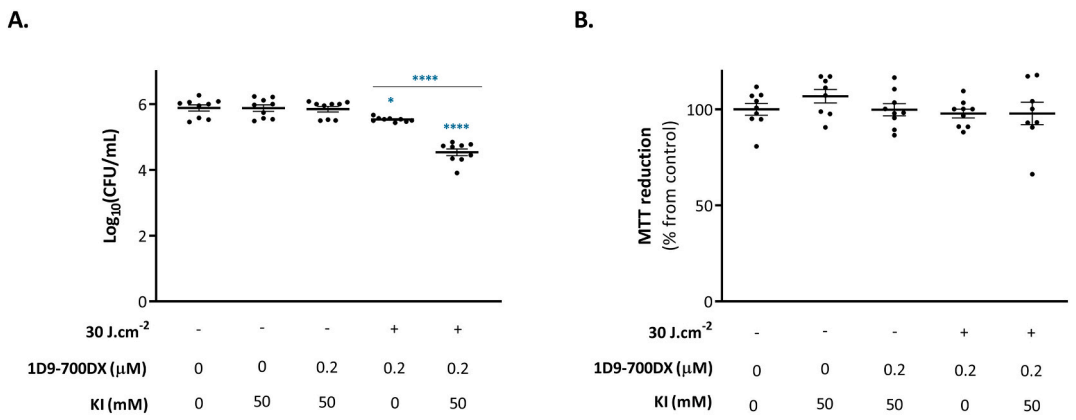

Fig. 6. (Photo-)cytotoxicity of 1D9-700DX towards MRSA-infected HeLa cells. **A.** CA-MRSA AH4807 was grown to exponential phase in RPMI medium and incubated with 30,000 HeLa cells (MOI = 10), 0.15 μM of 1D9-700DX and/or PBS and/or KI (50 mM). After 30 min incubation, cells were either irradiated with red light (30 J·cm^{-2}) or kept in the dark. Numbers of surviving bacteria (Log_{10}[CFU/mL]) are represented in the Fig. **B.** (Photo-)cytotoxicity was assessed using the colorimetric MTT assay 24 h after treatment. The percentage of cell viability was calculated relative to viable control cells that were infected with MRSA and mock-treated with PBS in the dark. Cells treated with 1% SDS were used as a control for cell killing. Data are presented as mean ± SEM of three independent experiments performed in triplicates. Ordinary one-way ANOVA tests with subsequent Holm-Sidak's multiple-comparison tests were used for statistical analysis. Significant differences compared with the control group (no photosensitizer, no light and no KI) are marked with blue asterisks as follows: *$P < 0.03$; ****$P < 0.0001$.

with red light, produces sufficient ROS to kill MRSA [22]. However, the efficacy of aPDT with the 1D9-700DX immunoconjugate is challenged by antioxidants in the host, as was exemplified by aPDT studies in human plasma [22]. Here, we sought to define the molecular basis of the aPDT-antagonizing activity in plasma and to optimize a KI-based approach for enhancing the bactericidal impact of aPDT with 1D9-700DX.

Previous research has shown that HSA is an important antioxidant that mediates the scavenging of ROS through its conserved Cys-34 residue which, in fact, represents the most abundant thiol portion in human plasma [28]. Oxidation of the free sulfhydryl group of Cys-34 leads to the formation of sulfenic acid, which is responsible for ROS scavenging [43]. Our present study shows that a 20-fold lower concentration of HSA compared to the HSA concentration in human plasma (i.e. ~43 mg·mL^{-1}) [44], can already completely block 1D9-700DX-mediated aPDT against CA-MRSA. Importantly, we show that HSA's antioxidant activity can be inhibited by the alkylating agents IAA and NEM, which react with free thiols and monitor changes in the redox state of proteins [45,46]. Thus, we were able to correlate free thiols of HSA in our experimental setup to the efficacy of aPDT with 1D9-700DX. The important conclusion from these findings is that HSA represents a major aPDT-antagonizing factor in the eradication of MRSA.

Due to their general toxicity, alkylating agents cannot be applied to potentiate aPDT for clinical applications and, consequently, alternative solutions are needed to overcome antioxidant activities in the human host. Therefore, we evaluated the possible use of KI in the context of our targeted aPDT approach. The non-toxic inorganic salt KI has already been explored for the possible potentiation of non-targeted aPDT in the treatment of infections [27,47,48]. Importantly, saturated KI solutions have been approved by the US Food and Drug Administration (FDA) for oral administration to block the absorption of radioactive iodine-131 by the thyroid gland in case of radiation emergencies, and for the treatment of fungal infections, such as subcutaneous zygomycosis [49,50]. We previously showed that the combination of KI with 1D9-700DX allows the eradication of high loads of CA-MRSA, even in the presence of blood plasma [22]. In the present study, we employed a defined setup where plasma was replaced by HSA to determine the optimal concentrations of 1D9-700DX and KI for targeted aPDT to eradicate MRSA. Importantly, our findings show that the required concentration of our immunoconjugate can be reduced 6-fold for effective aPDT of CA-MRSA performed in the presence of 30 μM KI. This dose of KI is still ~13,000-fold below the FDA-approved KI dose of 130 mg of KI for adults weighing 70 kg or more [51]. Moreover, we show that the red light irradiation time may be halved in the presence of KI. We anticipate that the optimization of these aPDT settings in terms of agent concentration and red light exposure will be instructive for the possible clinical translation of aPDT with 1D9-700DX, as it will minimize possible damage to the tissues surrounding a site of infection [39]. Moreover, lower doses of a photosensitizer allow faster clearance from the body, which can reduce skin photosensitivity from weeks to days [52]. As new iodine-reactive species result from the reaction of KI with the $^1O_2$ produced upon aPDT, it was also necessary to evaluate whether our aPDT approach with 1D9-700DX still targets MRSA specifically. Indeed, this is the case, as demonstrated by negligible side effects towards other non-targeted co-cultured bacteria and mammalian cells. This shows that, also in the presence of the non-targeted KI, the immunoconjugate 1D9-700DX retains its target specificity for *S. aureus*.

Altogether, we conclude that the antioxidant activity of HSA towards the ROS produced upon aPDT with 1D9-700DX can be overcome by the application of KI. Moreover, in the presence of this inorganic salt it is possible to drastically reduce both the immunoconjugate concentration and irradiation time. Importantly, the iodine and ROS produced upon aPDT with 1D9-700DX combined with KI, selectively kill the targeted bacteria without affecting surrounding cells and other bacteria. Our findings thus suggest that targeted aPDT with bacteria-specific photoactivatable immunoconjugates that produce high yields of singlet oxygen, such as 1D9-700DX, represents a promising approach that may complement the currently applied antimicrobial therapy of MRSA infections. Conceivably, a combination of aPDT with KI, if applied topically, may be implemented in future treatments of skin or implant-associated infections. In particular, infected implants often need to be removed by revision surgery with debridement of surrounding infected tissue if conventional antibiotic therapy fails. In such a surgical setting, aPDT may have added therapeutic value, because it could be applied to eliminate any residual bacteria. However, the presence of blood around the infected implant and tissue would limit the efficacy of the aPDT due to the antioxidant activity of HSA. Here, the topical administration of KI may serve to enhance the efficacy of aPDT for eliminating the targeted infectious microorganisms, as evidenced in the present study.

4. Materials and Methods

4.1. Conjugation of the 1D9 Monoclonal Antibody with IRDye 700DX-NHS

The human mAb 1D9 was produced as previously described [18] by transient transfection of Expi293F cells (Life Technologies). IRDye® 700DX (LiCor Biosciences) was cross-linked to the human mAb 1D9 via activated N-hydroxysuccinimide ester chemistry according to the manufacturer's instructions.

4.2. Effect of Human Plasma on 1D9-700DX Integrity

1D9-700DX was incubated with or without CA-MRSA for 30 min, followed by incubation with human plasma for 90 min, at 37 °C, under shaking. LDS-PAGE analysis of the 1D9-700DX immunoconjugate was performed using a 10% Bis-Tris gel (NuPAGE gels, Life Technologies) followed by fluorescence imaging with an Amersham™ Typhoon™ Biomolecular Imager (GE Healthcare). A reducing agent (NuPAGE, ThermoFisher) was employed to separate the heavy and light chains, and to improve the band resolution.

4.3. Evaluation of the Antioxidant Capacity of Different Serum Albumins

The CA-MRSA strain AH4807 was derived from the CA-MRSA LAC strain AH126353, where the *P. luminescens lux* operon was modified for Gram-positive bacterial expression and integrated at the φ11 attachment site on a plasmid of the host strain [53]. Bacteria were grown in Tryptic Soy Broth (TSB) to exponential phase (OD_{600} = 0.5) as previously described by Bispo et al. [22]. The bacteria were 10-fold diluted and 50 μL aliquots (~2×10^7 CFU/ml) were incubated with 50 μL of a cocktail mixture of 1D9-700DX (3.3 μM) or PBS and/or HSA or BSA (Sigma-Aldrich; 1.3, 2.5 and 5 mg·mL^{-1}) in a 96-well plate in the dark for 30 min at room temperature (RT). Afterwards, bacteria were illuminated with a high-output LED device that emits red light at 690 nm, at a radiance of 30 J.cm^{-2} (100 mW·cm^{-2}, 5 min) [54]. After treatment, bacteria were serially diluted in PBS, plated on blood-agar (BA) plates and then incubated aerobically for 16 h at 37 °C for CFU counting.

4.4. Blocking Thiols of Serum Albumins with Iodoacetamide or N-ethylmaleimide

To determine whether blocking free thiols of serum albumin can restore the aPDT effect, HSA or BSA were incubated with the alkylating agents IAA or NEM. First, toxicity dose-response studies with 2-fold increasing concentrations of IAA (Sigma-Aldrich) or NEM (Sigma-Aldrich) and the CA-MRSA strain were conducted. After determining the highest concentrations of NEM and IAA that are not toxic to this *S. aureus* strain, 50 μL (≈2×10^7 CFU/ml) bacterial suspensions were incubated with 50 μL of mixtures of 1D9-700DX (1.5 or 3.3 μM) or PBS, in the presence or absence of HSA or BSA (1.3 mg·mL^{-1}) and with or without IAA or NEM (0.8 and 0.3 mg·mL^{-1}, respectively), in the dark for 30 min at RT. Following incubation, bacteria were illuminated with 30 J·cm^{-2} of red light. After treatment, bacteria were serially diluted in PBS, plated on BA plates and then incubated aerobically for 16 h at 37 °C for CFU counting.

4.5. Quantification of Reduced Thiol Groups of HSA

The assay for thiol measurement in native HSA in the absence of presence of NEM was adapted from the Ellman's assay [37], following the recommendations by Tong et al. [55]. In this assay, 5,5′-dithiobis, 2-nitrobenzoic acid (DTNB, Thermo Scientific™) will react with free thiols in HSA, resulting in the formation of 2-nitro-5-thiobenzoate (TNB^-) by disulphide bond cleavage and subsequent formation of TNB^{2-} [37]. 100 μL of HSA (0.03–0.5 mg·mL^{-1}) were incubated with 100 μL PBS and/or 1.2 mg·mL^{-1} of NEM [45,55] prepared in ethanol in a 96-well plate for 30 min. Hundred microlitres of aliquots from this mixture were then transferred to separate wells and incubated for 15 min with 100 μL of 14 mM DTNB prepared in ethanol. The generation of TNB^{2-} was monitored by reading the absorbance at 412 nm with a microplate spectrophotometer (Synergy™ HT, Biotek instruments). Each experiment was performed in triplicate at least three times.

4.6. Potentiation of 1D9-700DX-aPDT with Potassium Iodide

Bacterial suspensions (2×10^7 CFU/mL) of CA-MRSA AH4807 were incubated with several concentrations of KI (7.5, 15 and 30 μM; Sigma-Aldrich) or PBS and 1.5 μM of 1D9-700DX or PBS to determine the optimal KI concentration to eradicate the bacteria. After 30 min incubation in the dark, at RT, bacteria were irradiated with 30 J·cm^{-2} of red light. To determine the optimal irradiation dosage, 120 μM of KI were incubated with the bacteria and 1D9-700DX, for 30 min, at RT, in the dark. Afterwards the samples were subjected to red light at a radiance exposure that ranged between 0 and 30 J·cm^{-2}. To assess the ability of KI to rescue the aPDT effect in the presence of HSA, CA-MRSA was incubated with mixtures of 1D9-700DX or PBS, and/or KI or PBS, and/or HSA (1.3 mg·mL^{-1}) and kept in the dark for 30 min, at RT. Bacteria were subsequently illuminated with 30 J·cm^{-2} of red light. Lastly, the bacteria were serially diluted in PBS, plated on BA plates and then incubated aerobically for 16 h at 37 °C for CFU counting.

4.7. 1D9-700DX aPDT Combined with KI in a Co-culture of S. aureus and K. oxytoca

Clinical isolates of *S. aureus* and *K. oxytoca* obtained from a used bandage from a chronic wound of a Dutch patient with Junctional EB [41] were grown overnight in TSB under vigorous shaking at 37 °C. The cultures were then diluted to an OD_{600} of 0.1 in TSB and grown to exponential phase (OD_{600} = 0.5) for 1.5 h. Monocultures were started with an initial OD_{600} of 0.05 while co-cultures were inoculated with an OD_{600} of 0.025 of each isolate to a total of 0.05. After centrifugation of 150 μL of bacterial mono- or co-cultures, at 16,200 ×*g* for 2 min, the collected bacterial cells were incubated with 1.5 μM of 1D9-700DX, for 30 min, at RT. The bacteria were washed once with PBS to remove the unbound conjugate and the pellet was further resuspended in 150 μL of PBS with or without 30 μM of KI. The bacteria were then transferred to a 96-well plate for irradiation with red light, at 30 J·cm^{-2}. After this treatment, the bacteria were serially diluted in PBS, plated on BA plates and then incubated aerobically for 16 h at 37 °C for CFU counting.

4.8. Toxicity of KI Towards HeLa Cells

The human cervical cancer HeLa cell line (ATCC) was cultured in Dulbecco's Modified Eagle Medium (DMEM)-GlutaMAX medium (Gibco™) supplemented with 10% of fetal bovine serum (Gibco™) at 37 °C and 5% CO_2. 0.25% Trypsin-EDTA (Gibco™) was used to detach adherent cells for subculturing. Cells were then seeded into 96-well cell culture plates at a density of 3×10^4 cells/well. Twenty-four hours after seeding, 3×10^4 cells were incubated with 2-fold increasing concentrations of KI (up to 100 mM) for 30 min. Metabolic activity of the HeLa cells was subsequently determined with the MTT assay, which measures the cells' ability to reduce MTT (Sigma-Aldrich) to colored formazan crystals. To this end, the cells were washed twice with Dulbecco's phosphate-buffered saline (DPBS), and incubated with 0.5 mg·mL^{-1} of MTT for 3 h, at 37 °C and 5% CO_2. The formation of formazan was quantified with a microplate spectrophotometer (Synergy™ HT, Biotek Instruments) by measuring the absorbance at 570 nm, using 620 nm as the background wavelength. The percentage of absorbance for each treated sample was normalized to each untreated control. Each experiment was performed in triplicate at least three times.

4.9. (Photo-)cytotoxicity of 1D9-700DX Against MRSA-infected HeLa Cells

HeLa cells were cultured and seeded as described above. 24 h after seeding, the cells were infected with 50 μL of CA-MRSA AH4807 with a multiplicity of infection of 10. Figty microlitres of 1D9-700DX (0.2 μM) or DPBS), and KI (50 mM) or DPBS were also added to the cells in the dark, for 30 min. Irradiation with 30 $J{\cdot}cm^{-2}$ of red light was subsequently performed. The bacteria present in the supernatant were serially diluted in PBS, plated on BA plates and then incubated aerobically for 16 h at 37 °C for CFU counting. Cell metabolic activity upon aPDT was determined with the MTT assay as described above.

4.10. Statistics

The results are presented as the mean ± the standard error of the mean (S.E.M.). All statistical analyses were performed with GraphPad Prism 8.0.1. Variables in three or more unmatched groups were assessed with Kruskal-Wallis tests and subsequently by the Dunn's or the Dunnett's multiple comparisons tests or Ordinary one-way ANOVA with a subsequent Holm-Sidak's multiple-comparison test depending on the Gaussian distribution of residues. *P*-values <0.05 were considered significant.

4.11. Study Approval

Blood donations from healthy volunteers were collected with approval of the medical ethics committee of the UMCG (approval n° METc 2016/621) and after written informed consent, in accordance to the Helsinki Guidelines and local regulations.

Funding Statement

M.B. was supported by the EU Horizon 2020 Programme under the Marie Skłodowska-Curie grant agreement 713660 (Pronkjewail). S.S. was supported with a Talent Grant from The Eric Bleumink Fund (EBF) of the University of Groningen.

Declaration of Competing Interest

J.M.v.D. has filed a patent application on the use of monoclonal antibody 1D9 for infection imaging, which is owned by his employer University Medical Center Groningen. The other authors have nothing to disclose.

Acknowledgements

We thank Marina López-Álvarez for helpful discussions and technical support.

Appendix A. Supplementary Data

Supplementary data to this article can be found online at https://doi.org/10.1016/j.jphotobiol.2021.112334.

References

[1] G.K. Paterson, E.M. Harrison, M.A. Holmes, The emergence of mecC methicillin-resistant *Staphylococcus aureus*, Trends Microbiol. 22 (1) (2014) 42–47.
[2] P. Kale, B. Dhawan, The changing face of community-acquired methicillin-resistant *Staphylococcus aureus*, Indian J. Med. Microbiol. 34 (3) (2016) 275–285.
[3] F.A. Orrett, M. Land, Methicillin-resistant Staphylococcus aureus prevalence: current susceptibility patterns in Trinidad, BMC Infect. Dis. 6 (2006) 83.
[4] X. Shi, C.Y. Zhang, J. Gao, Z. Wang, Recent advances in photodynamic therapy for cancer and infectious diseases, Wiley Interdiscip. Rev. Nanomed. Nanobiotechnol. 11 (5) (2019), e1560.
[5] M. Wainwright, T. Maisch, S. Nonell, K. Plaetzer, A. Almeida, G.P. Tegos, et al., Photoantimicrobials—are we afraid of the light? Lancet Infect. Dis. 17 (2) (2017) e49–e55.
[6] Y. Liu, R. Qin, S.A.J. Zaat, E. Breukink, M. Heger, Antibacterial photodynamic therapy: overview of a promising approach to fight antibiotic-resistant bacterial infections, J. Clin. Transl. Res. 1 (3) (2015) 140–167.
[7] A. Tavares, C.M.B. Carvalho, M.A. Faustino, M.G.P.M.S. Neves, J.P.C. Tomé, A. C. Tomé, et al., Antimicrobial photodynamic therapy: study of bacterial recovery viability and potential development of resistance after treatment, Mar. Drugs 8 (1) (2010) 91–105.
[8] N. Kashef, M.R. Hamblin, Can microbial cells develop resistance to oxidative stress in antimicrobial photodynamic inactivation? Drug Resist. Updat. 31 (2017) 31–42.
[9] X.-J. Fu, Y. Fang, M. Yao, Antimicrobial photodynamic therapy for methicillin-resistant *Staphylococcus aureus* infection, Biomed. Res. Int. 2013 (2013) 159157.
[10] A. Dreisbach, J.M. van Dijl, G. Buist, The cell surface proteome of *Staphylococcus aureus*, Proteomics. 11 (15) (2011) 3154–3168.
[11] M.M. Van Der Kooi-Pol, C.P. De Vogel, G.N. Westerhout-Pluister, Y.K. Veenstra-Kyuchukova, J.C. Duipmans, C. Glasner, et al., High anti-staphylococcal antibody titers in patients with epidermolysis bullosa relate to long-term colonization with alternating types of staphylococcus aureus, J. Invest. Dermatol. 133 (3) (2013) 847–850.
[12] U. Lorenz, K. Ohlsen, H. Karch, M. Hecker, A. Thiede, J. Hacker, Human antibody response during sepsis against targets expressed by methicillin resistant *Staphylococcus aureus*, FEMS Immunol. Med. Microbiol. 29 (2) (2000) 145–153.
[13] M.J.J.B. Sibbald, A.K. Ziebandt, S. Engelmann, M. Hecker, A. de Jong, H.J. M. Harmsen, et al., Mapping the pathways to staphylococcal pathogenesis by comparative Secretomics, Microbiol. Mol. Biol. Rev. 70 (3) (2006) 755–788.
[14] A.K. Ziebandt, H. Kusch, M. Degner, S. Jaglitz, M.J.J.B. Sibbald, J.P. Arends, et al., Proteomics uncovers extreme heterogeneity in the *Staphylococcus aureus* exoproteome due to genomic plasticity and variant gene regulation, Proteomics. 10 (8) (2010) 1634–1644.
[15] A. Dreisbach, M. Wang, M.M. van der Kooi-Pol, E. Reilman, D.G.A.M. Koedijk, R.A. T. Mars, et al., Tryptic shaving of *Staphylococcus aureus* unveils immunodominant epitopes on the bacterial cell surface, J. Proteome Res. 19 (8) (2020) 2997–3010.
[16] U. Lorenz, B. Lorenz, T. Schmitter, K. Streker, C. Erck, J. Wehland, et al., Functional antibodies targeting IsaA of *Staphylococcus aureus* augment host immune response and open new perspectives for antibacterial therapy, Antimicrob. Agents Chemother. 55 (1) (2011) 165–173.
[17] B. Oesterreich, B. Lorenz, T. Schmitter, R. Kontermann, M. Zenn, B. Zimmermann, et al., Characterization of the biological anti-staphylococcal functionality of hUK-66 IgG1, ahumanized monoclonal antibody as substantial component for an immunotherapeutic approach, Hum. Vaccines Immunother. 10 (4) (2014) 926–937.
[18] S. van den Berg, H.P.J. Bonarius, K.P.M. van Kessel, G.S. Elsinga, N. Kooi, H. Westra, et al., A human monoclonal antibody targeting the conserved staphylococcal antigen IsaA protects mice against *Staphylococcus aureus* bacteremia, Int. J. Med. Microbiol. 305 (1) (2015) 55–64.
[19] F. Romero Pastrana, J.M. Thompson, M. Heuker, H. Hoekstra, C.A. Dillen, R. V. Ortines, et al., Noninvasive optical and nuclear imaging of Staphylococcus-specific infection with a human monoclonal antibody-based probe, Virulence 9 (1) (2018) 262–272.
[20] S.D. Zoller, H.Y. Park, T. Olafsen, C. Zamilpa, Z.D.C. Burke, G. Blumstein, et al., Multimodal imaging guides surgical management in a preclinical spinal implant infection model, JCI Insight 4 (3) (2019), e124813.
[21] W.L. Sheppard, G.M. Mosich, R.A. Smith, C.D. Hamad, H.Y. Park, S.D. Zoller, et al., Novel in vivo mouse model of shoulder implant infection, J. Shoulder Elb. Surg. 29 (7) (2020) 1412–1424.
[22] M. Bispo, A. Anaya-Sanchez, S. Suhani, E.J.M. Raineri, M. López-Álvarez, M. Heuker, et al., Fighting *Staphylococcus aureus* infections with light and photoimmunoconjugates, JCI Insight 5 (22) (2020), e139512.
[23] M. Mitsunaga, M. Ogawa, N. Kosaka, L.T. Rosenblum, P.L. Choyke, H. Kobayashi, Cancer cell-selective in vivo near infrared photoimmunotherapy targeting specific membrane molecules, Nat. Med. 17 (12) (2011) 1685–1691.
[24] M.A. Biel, A.M. Gillenwater, D.M. Cognetti, J.M. Johnson, A. Argiris, M. Tahara, A global phase III multicenter, randomized, double-arm, open label trial of ASP-1929 photoimmunotherapy versus physician's choice standard of care for the treatment of patients with locoregional, recurrent head and neck squamous cell carcinoma (rHNSCC), J. Clin. Oncol. 37 (15) (2019). TPS6094–TPS6094.
[25] D. Mew, C.K. Wat, G.H. Towers, J.G. Levy, Photoimmunotherapy: treatment of animal tumors with tumor-specific monoclonal antibody-hematoporphyrin conjugates, J. Immunol. 130 (3) (1983) 1473–1477.
[26] W. Xuan, Y. He, L. Huang, Y.Y. Huang, B. Bhayana, L. Xi, et al., Antimicrobial photodynamic inactivation mediated by tetracyclines in vitro and in vivo: photochemical mechanisms and potentiation by potassium iodide, Sci. Rep. 8 (2018) 17130.
[27] C. Vieira, A.T.P.C. Gomes, M.Q. Mesquita, N.M.M. Moura, G.P.M.S. Neves, A. F. Faustino, et al., An insight into the potentiation effect of potassium iodide on APDT efficacy, Front. Microbiol. 9 (2018) 2665.
[28] M. Taverna, A.L. Marie, J.P. Mira, B. Guidet, Specific antioxidant properties of human serum albumin, Ann. Intensive Care 3 (1) (2013) 4.
[29] X. Dong, R. Zhou, H. Jing, Characterization and antioxidant activity of bovine serum albumin and sulforaphane complex in different solvent systems, J. Lumin. 146 (2014) 351–357.
[30] R. Boöttger, R. Hoffmann, D. Knappe, Differential stability of therapeutic peptides with different proteolytic cleavage sites in blood, plasma and serum, PLoS One 12 (6) (2017), e0178943.

[31] J. Vaughan, R. Benson, K. Vaughan, Assessing the effectiveness of antimicrobial wound dressings in vitro, in: Advanced Wound Repair Therapies, Woodhead Publishing Series in Biomaterials, 2011, pp. 227–246.
[32] S. Suttapitugsakul, H. Xiao, J. Smeekens, R. Wu, Evaluation and optimization of reduction and alkylation methods to maximize peptide identification with MS-based proteomics, Mol. BioSyst. 13 (12) (2017) 2574–2582.
[33] N. Linzner, V. Van Loi, V.N. Fritsch, H. Antelmann, Thiol-based redox switches in the major pathogen *Staphylococcus aureus*, Biol. Chem. 402 (3) (2021) 333–361.
[34] Y. Akdogan, J. Reichenwallner, D. Hinderberger, Evidence for water-tuned structural differences in proteins: an approach emphasizing variations in local hydrophilicity, PLoS One 7 (9) (2012), e45681.
[35] K. Oettl, R.E. Stauber, Physiological and pathological changes in the redox state of human serum albumin critically influence its binding properties, Br. J. Pharmacol. 151 (5) (2007) 580–590.
[36] B. Subhadra, S. Surendran, D.H. Kim, K. Woo, M.H. Oh, C.H. Choi, The transcription factor NemR is an electrophile-sensing regulator important for the detoxification of reactive electrophiles in *Acinetobacter nosocomialis*, Res. Microbiol. 170 (3) (2019) 123–130.
[37] G.L. Ellman, Tissue sulfhydryl groups, Arch. Biochem. Biophys. 82 (1) (1959) 70–77.
[38] M.R. Hamblin, H. Abrahamse, Inorganic salts and antimicrobial photodynamic therapy: mechanistic conundrums? Molecules 23 (12) (2018) 3190.
[39] S. Rajesh, E. Koshi, K. Philip, A. Mohan, Antimicrobial photodynamic therapy: an overview, J. Indian Soc. Periodontol. 15 (4) (2011) 323–327.
[40] Environmental Protection Agency, Programs UEPAO of P. Standard Operating Procedure for AOAC Use Dilution Method for Testing Disinfectants, Jan 17, 2020, https://www.epa.gov/sites/default/files/2020-02/documents/mb-05-16.pdf (Accessed August 2021).
[41] A.N. García-Pérez, A. de Jong, S. Junker, D. Becher, M.A. Chlebowicz, J. C. Duipmans, et al., From the wound to the bench: exoproteome interplay between wound-colonizing *Staphylococcus aureus* strains and co-existing bacteria, Virulence 9 (1) (2017) 1–35.
[42] T.L. Riss, R.A. Moravec, A.L. Niles, S. Duellman, H.A. Benink, T.J. Worzella, et al., Cell viability assays, in: Assay Guidance Manual, Eli Lilly & Company and the National Center for Advancing Translational Sciences, 2004.
[43] M. Roche, P. Rondeau, N.R. Singh, E. Tarnus, E. Bourdon, The antioxidant properties of serum albumin, FEBS Lett. 582 (13) (2008) 1783–1787.
[44] M. Hassan, E. Azzazy, R.H. Christenson, et al., Clin. Chem. 43 (10) (1997) 2014a–2015.
[45] E. Bourdon, N. Loreau, L. Lagrost, D. Blache, Differential effects of cysteine and methionine residues in the antioxidant activity of human serum albumin, Free Radic. Res. 39 (1) (2005) 15–20.
[46] S.L. Cuddihy, J.W. Baty, K.K. Brown, C.C. Winterbourn, M.B. Hampton, Proteomic detection of oxidized and reduced thiol proteins in cultured cells, Methods Mol. Biol. 519 (2009) 363–375.
[47] X. Wen, X. Zhang, G. Szewczyk, A. El-Hussein, Y.-Y. Huang, T. Sarna, et al., Potassium iodide potentiates antimicrobial photodynamic inactivation mediated by Rose Bengal in in vitro and in vivo studies, Antimicrob. Agents Chemother. 61 (7) (2017), e00467-17.
[48] D. Vecchio, A. Gupta, L. Huang, G. Landi, P. Avci, A. Rodas, et al., Bacterial photodynamic inactivation mediated by methylene blue and red light is enhanced by synergistic effect of potassium iodide, Antimicrob. Agents Chemother. 59 (9) (2015) 5203–5212.
[49] V. Mendiratta, S. Karmakar, A. Jain, M. Jabeen, Severe cutaneous zygomycosis due to basidiobolus ranarum in a young infant, Pediatr. Dermatol. 29 (1) (2012) 121–123.
[50] Guidance Potassium Iodide as a Thyroid Blocking Agent in Radiation Emergencies. Food and Drug Administration. Dec 2000. https://www.nrc.gov/docs/ML0109/ML010950195.pdf. (Accessed August 2021).
[51] M. Milczarek, J. Stepniak, A. Lewinski, M. Karbownik-Lewinska, Potassium iodide, but not potassium iodate, as a potential protective agent against oxidative damage to membrane lipids in porcine thyroid, Thyroid. Res. 6 (2013) 10.
[52] D. van Straten, V. Mashayekhi, H.S. de Bruijn, S. Oliveira, D.J. Robinson, Oncologic photodynamic therapy: basic principles, current clinical status and future directions, Cancers (Basel) 9 (2) (2017) 19.
[53] R.J. Miller, H.A. Crosby, K. Schilcher, Y. Wang, R.V. Ortines, M. Mazhar, et al., Development of a *Staphylococcus aureus* reporter strain with click beetle red luciferase for enhanced in vivo imaging of experimental bacteremia and mixed infections, Sci. Rep. 9 (1) (2019) 1–19.
[54] E. de Boer, J.M. Warram, E. Hartmans, P.J. Bremer, B. Bijl, L.M. Crane, et al., A standardized light-emitting diode device for photoimmunotherapy, J. Nucl. Med. 55 (11) (2014) 1893–1898.
[55] L.M. Tong, S. Sasaki, D.J. McClements, E.A. Decker, Mechanisms of the antioxidant activity of a high molecular weight fraction of whey, J. Agric. Food Chem. 48 (5) (2000) 1473–1478.